STABILITY STUDY OF RAYLEIGH'S PROFILE

Ruth Moorman

Report Submitted August 24, 2018
Assignment 1 for EMSC4050 *Instabilities in Fluids*
Research School of Earth Sciences, Australian National University
u5808670@anu.edu.au

1. BASIC STATE

In this first independent investigation of the course, I will analyse the modal stability of the 2 dimensional Rayleigh Profile, a steady state solution of the Boussinesq flow equations described by the following piecewise continuous velocity field in a constant density medium,

$$\mathbf{u} = U(z)\hat{\mathbf{x}} = \begin{cases} U_0\hat{\mathbf{x}} & z > a \\ \frac{U_0}{a} z\hat{\mathbf{x}} & -a < z < a \\ -U_0\hat{\mathbf{x}} & z < a \end{cases}, \qquad \rho = \rho(z) = \rho_0. \quad (1)$$

Here U_0, ρ_0 and a are constants, with $2a$ representing the length of the shear zone, and the domain is infinite in x and z as pictured in Figure 1. This basic state is one of a family of fixed point solutions to the Boussinesq equations referred to as parallel shear flows (introduced in the lectures), which take the form,

$$\mathbf{u} = U(z)\hat{\mathbf{x}}, \quad \rho = \rho(z). \quad (2)$$

Herein I will use both analytical (Section 2) and numerical (Section 3) methods to characterise the *modal* stability (stability or instability at $t \to \infty$) of this basic state by approaching the time dependence of the flow as an eigenvalue problem.

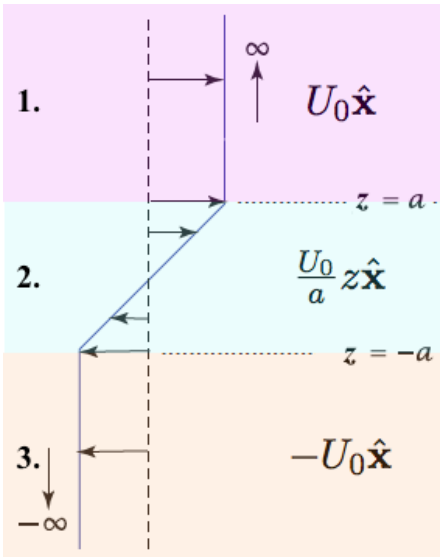

Figure 1: The Rayleigh flow basic state. Shading and labelling highlights 3 sections separated by discontinuities in ω and $U'(z)$. Figure adapted from Vallis (2017).

2. ANALYTICAL STABILITY ANALYSIS

If we consider the velocity field in Equation 1, we can compute its vorticity ($\boldsymbol{\omega}$) to be,

$$\boldsymbol{\omega} = \begin{cases} \nabla \times U_0\hat{\mathbf{x}} = 0 & z > a \\ \nabla \times \frac{U_0}{a} z\hat{\mathbf{x}} = \frac{U_0}{a}\hat{\mathbf{y}} & -a < z < a \\ \nabla \times -U_0\hat{\mathbf{x}} = 0 & z < -a \end{cases} \quad (3)$$

and note that there exists two discontinuities in $\boldsymbol{\omega}$ at $z = \pm a$. These discontinuities in $\boldsymbol{\omega}$ coincide with discontinuities in $U'(z)$ and suggest that the system contains 2 internal 'boundaries' that should be accounted for in our characterisation of the flow. Hence it is convenient to segment our flow into 3 interacting regions (1, 2, 3 in Figure 1) when analysing the system analytically.

After segmenting the problem thus, the procedure followed for the analytical analysis is:

1. Introduce an infinitesimal perturbation ϕ' (which collectively represents all the perturbation fields) to the basic state and assume its solution is of the form,

$$\phi' = \begin{bmatrix} \psi_i' \\ p_i' \\ \eta_j' \end{bmatrix} = \begin{bmatrix} \hat{\psi}_i(z) \\ \hat{p}_i(z) \\ \hat{\eta}_j(z) \end{bmatrix} e^{ikx+\sigma t} = \hat{\phi}(z) e^{ikx+\sigma t} \tag{4}$$

   where $i \in \{1, 2, 3\}$ refers to the flow segments and $j \in \{1, 2\}$ refers to the interfaces between the flow segments. Here we use the fact that our perturbation is translationally invariant in x and t to introduce exponential solutions in these terms (note k here is the real x component wavenumber of our perturbation and σ is the growth rate of the perturbation) whilst the nature of the z dependence is yet to be determined. The perturbation velocity fields u', w' are captured in the stream function ψ' as is appropriate for 2 dimensional flows under the Boussinesq approximation. We define,

$$u' = -\partial_z \psi', \quad w' = \partial_x \psi' \tag{5}$$

   throughout the analysis, and denote the displacement of the interfaces between flow layers upon perturbation as η_j'.

2. Characterise the boundary conditions that the perturbation field ϕ' should obey (at each segment interface and at the domain edges).

3. Determine the equations of motion the perturbation field ϕ' should obey (in each segment).

4. Combine the information from the boundary conditions and the equations of motion to place constraints on the value of σ, the growth rate of the perturbation ϕ'.

This is equivalent to obtaining solutions to the eigenvalue problem,

$$\partial_t \phi' = \mathcal{A} \phi' \tag{6}$$

of the form given in Equation 4.

2.1. Boundary Conditions

The most simple boundary condition that we may prescribe is that the infinitesimal perturbations decay as we move far away from the shear zone, i.e.,

$$| \psi' | \to 0 \quad \text{as} \quad | z | \to \infty. \tag{7}$$

On its own, however, this condition is insufficient. We also require that pressure is continuous across the layer interfaces, and that these interfaces, which are lines of constant $\boldsymbol{\omega}$, behave as material lines. These latter boundary conditions may be manipulated to impose constraints on ψ'.

2.1.1. Pressure Continuity

Pressure continuity requires that, $P_0 - \rho(z) g z + p'(z)$ is continuous across layer interfaces, which, in this constant ρ environment, simply requires that, p' is continuous across interfaces.

In order to use this condition to constrain ψ', we take the momentum equation in the x direction (parallel to the interfaces) in terms of stream functions,

$$-\partial_{tz}\psi' - U(z)\partial_{xz}\psi' + \partial_x \psi' \partial_z U(z) = -\partial_x p' \tag{8}$$

and assume solutions of the form given in Equation 4 to obtain the expression (following some algebra and a few applications of the chain rule),

$$-\Big[\sigma + ikU(z)\Big]\partial_z \hat{\psi} + ikU'(z)\hat{\psi} = -ik\hat{p}. \tag{9}$$

Now, we have that $\hat{p}$ and thus the RHS of Equation 9 is continuous across interfaces, and so it must be that the LHS of Equation 9 is also continuous across interfaces, constraining ψ' as desired.

2.1.2. *Material Interfaces*

We require that the ω discontinuities behave as material lines. Conservation of the normal velocity across these material lines requires (here I skip over a derivation covered in the lectures that involves some linearisations) that,

$$\frac{D}{Dt}\eta' = w' \tag{10}$$

is conserved across these lines. i.e.

$$\partial_t \eta' + U(z)\partial_x \eta' = \partial_x \psi' \tag{11}$$

or, assuming exponential solutions in Equation 4,

$$\Big[\sigma + U(z)ik\Big]\hat{\eta} = ik\hat{\psi} \tag{12}$$

is conserved across interfaces. This implies the quantity,

$$\frac{ik\hat{\psi}}{\sigma + U(z)ik} \tag{13}$$

is conserved across $z = \pm a$. Since we have a continuous velocity profile in z, this simplifies to the condition that $\hat{\psi}$ is continuous across interfaces.

2.1.3. *Boundary Conditions Summary*

Boundary Condition #1: $-\Big[\sigma + ikU(z)\Big]\partial_z\hat{\psi} + ikU'(z)\hat{\psi}$ is continuous across $z = \pm a$

Boundary Condition #2: $\hat{\psi}$ is continuous across $z = \pm a$

Boundary Condition #3: $\mid \psi' \mid \to 0$ as $\mid z \mid \to \infty$

2.2. Equation of Motion

As was derived in the lectures, the Boussinesq equations for 2 dimensional parallel shear flows (i.e. steady states described by Equation 2) can be condensed into a single equation of motion, the *Rayleigh Equation*. When we assume solutions of ψ' of the form in Equation 4, the Rayleigh Equation simplifies to,

$$\sigma(\partial_{zz} - k^2) + U(z)ik(\partial_{zz} - k^2)\hat{\psi} - \partial_{zz}U(z)ik\hat{\psi} = 0. \tag{14}$$

Substituting in the expressions for $U(z)$ in the 3 flow layers gives us 3 equations of motion for the system,

$$\begin{array}{l} \sigma(\partial_{zz} - k^2)\hat{\psi}_1 + U_0 ik(\partial_{zz} - k^2)\hat{\psi}_1 = 0 \\ \sigma(\partial_{zz} - k^2)\hat{\psi}_2 + \frac{U_0 ikz}{a}(\partial_{zz} - k^2)\hat{\psi}_2 = 0 \\ \sigma(\partial_{zz} - k^2)\hat{\psi}_3 - U_0 ik(\partial_{zz} - k^2)\hat{\psi}_3 = 0 \end{array} \tag{15}$$

where subscripts refer to the 3 layers of flow in Figure 1. If we assume $\sigma + U_0 ik \neq 0$ ($z > a$), $\sigma + U_0 ikz/a \neq 0$ ($-a < z < a$), and $\sigma - U_0 ik \neq 0$ ($z < -a$), these differential equations simplify to,

$$\frac{\partial^2}{\partial z^2}\hat{\psi} - k^2\hat{\psi} = 0 \tag{16}$$

suggesting solutions of the form,

$$\hat{\psi} = \tilde{\psi}e^{\pm kz + c}. \tag{17}$$

When we consider the boundary conditions on ψ' at $\pm\infty$ and $\pm a$, namely that ψ' decays as z tends from $+a$ to $+\infty$ and from $-a$ to $-\infty$ and that ψ' is continuous across the $z = \pm a$ interfaces, we can deduce $\hat{\psi}$ takes the following form in our 3 layers,

$$\hat{\psi}_1 = Ae^{-k(z-a)} \tag{18}$$

$$\hat{\psi}_2 = Be^{k(z-a)} + Ce^{-k(z+a)} \tag{19}$$

$$\hat{\psi}_3 = De^{k(z+a)}. \tag{20}$$

Now we have a set of boundary conditions constraining $\hat{\psi}$, as well as the forms of $\hat{\psi}$ in each flow layer. The next step is to combine these strands to solve for σ, the growth rate of our perturbation field ϕ'.

2.3. Solving the stability eigenproblem (Analytical)

We construct a system of linear equations in A, B, C and D by substituting Equations 18-19 into Boundary Conditions #1 and #2.

At the upper interface ($z = a$), combining the boundary bonditions and equation of motion gives,

$$A\Big[\sigma + ikU_0\Big] = B\Big(- \Big[\sigma + ikU_0\Big] + \frac{U_0 i}{a}\Big) + Ce^{-2ka}\Big(\Big[\sigma + ikU_0\Big] + \frac{U_0 i}{a}\Big) \tag{21}$$

$$A = B + Ce^{-2ka} \tag{22}$$

whilst at the lower interface ($z = -a$) we have,

$$-D\Big[\sigma - ikU_0\Big] = Be^{-2ka}\Big(- \Big[\sigma - ikU_0\Big] + \frac{U_0 i}{a}\Big) + C\Big(\Big[\sigma - ikU_0\Big] + \frac{U_0 i}{a}\Big) \tag{23}$$

$$D = Be^{-2ka} + C. \tag{24}$$

Combing Equations 21-24 gives the following system,

$$\begin{bmatrix} (\sigma + ikU_0) & (\sigma + ikU_0) - \frac{U_0 i}{a} & -e^{-2ka}\big[(\sigma + ikU_0) + \frac{U_0 i}{a}\big] & 0 \\ 1 & -1 & -e^{-2ka} & 0 \\ 0 & e^{-2ka}\big[- (\sigma - ikU_0) + \frac{U_0 i}{a}\big] & (\sigma - ikU_0) + \frac{U_0 i}{a} & (\sigma - ikU_0) \\ 0 & -e^{-2ka} & -1 & 1 \end{bmatrix} \begin{bmatrix} A \\ B \\ C \\ D \end{bmatrix} = 0. \tag{25}$$

For this system to have non-trivial solutions, we require that the determinant of the 4×4 matrix is zero. So, for non-trivial solutions we must have a σ that satisfies,

$$\Big(2(\sigma - ikU_0) + \frac{U_0 i}{a}\Big)\Big(- 2(\sigma + ikU_0) + \frac{U_0 i}{a}\Big) + \Big(e^{-2ka}\frac{U_0 i}{a}\Big)\Big(- e^{-2ka}\frac{U_0 i}{a}\Big) = 0 \tag{26}$$

requiring,

$$\sigma = \pm\sqrt{-k^2U_0^2 + \frac{kU_0^2}{a} + \Big(\frac{U_0}{2a}\Big)^2(e^{-4ka} - 1)}. \tag{27}$$

From this we can see that the system has a real positive eigenvalue, implying growth of the perturbation field and thus modal instability, whenever the argument of the square root in Equation 27 is positive. This requires that whenever,

$$0 < ka <\sim 0.639 \tag{28}$$

holds, the basic state is modally unstable.

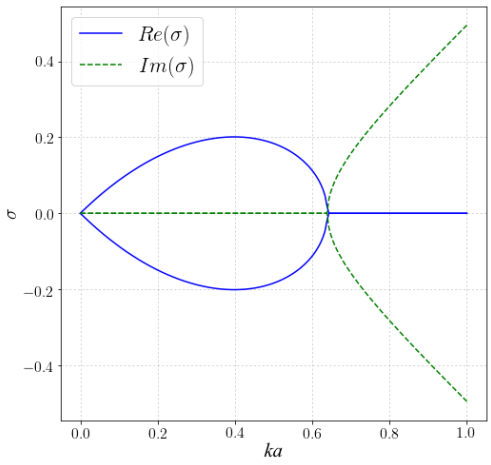

Figure 2: Dependence of the perturbation growth rate (σ) on the system lengthscale (ka) in the analytical solution.

The functional dependence of σ on the lengthscale ka is shown in Figure 2. The growth rate is purely real (containing a stable and unstable mode) for low ka until ka reaches the threshold value (Equation 28) where the growth rate becomes purely imaginary (and so stable). For very small values of ka, σ and ka are equal. This is corresponds to the eigenproblem solution for a Kelvin-Helmholtz profile, which this basic state approaches in the limit of $a \rightarrow 0$. The existence of such a sudden threshold between purely real and purely imaginary growth rates is intriguing and is discussed from the perspective of edge wave interactions in Section 4.

Perturbation flow fields associated with the stable ($Re(\sigma) < 0$) and unstable ($Re(\sigma) > 0$) eigenmodes at $ka = 0.4$ are visualised in Figure 3. In order to specify the flow fields, the constant B in Equation 19 was set to 1 and Equations 21-24 were used to constrain the values of A, C and D. This is necessary as the number of knowns in this system can only be used to constrain our perturbation solution down to a scaling factor. Note that the stable and unstable modes in Figure 3 are mirror images of one another. The unstable mode consists of perturbation streamfunctions that *lean into the mean flow,* whilst the stable mode consists of perturbations *aligning with the mean flow*. In both flows $\boldsymbol{\omega}$ is everywhere zero, a consequence of the piecewise linear nature of our mean velocity profile, and the interfacial displacements at the upper and lower interfaces (η') are slightly phase shifted with respect to one another.

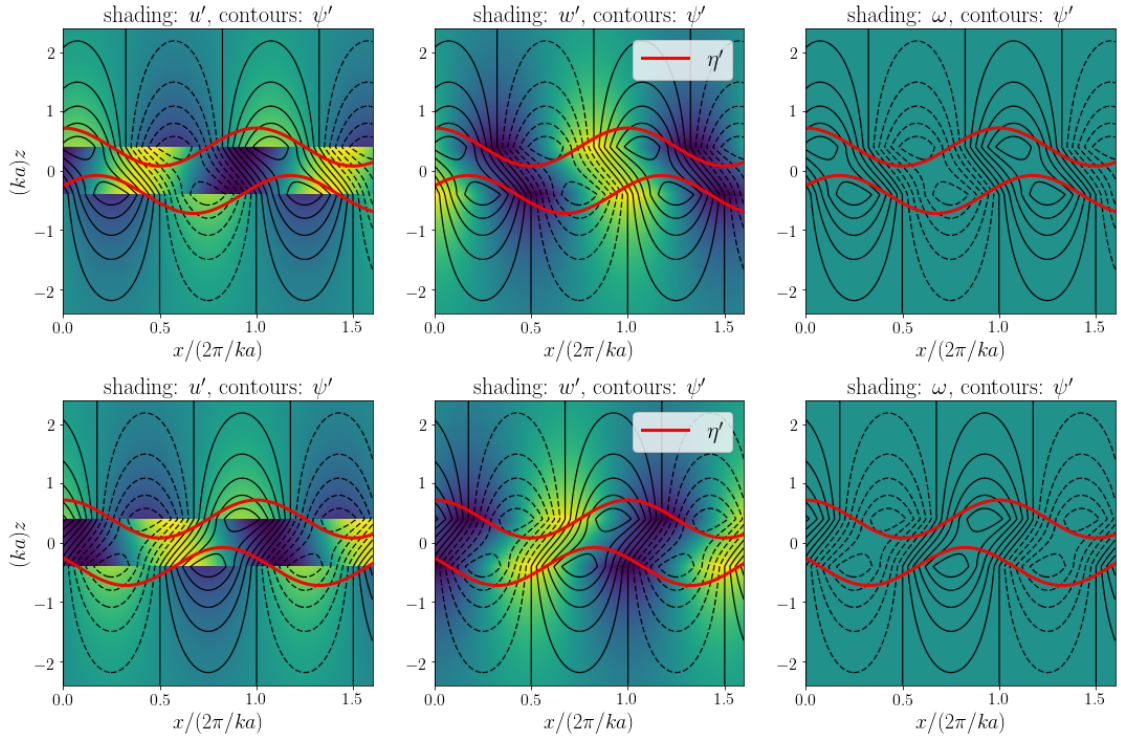

Figure 3: Plots of u', w', ψ' and $\boldsymbol{\omega}$ at $t = 0$ for complementary unstable (*top row*) and stable (*bottom row*) eigenmodes of the perturbation. Both plots show fields where $U_0 = a = 1$ and $ka = 0.4$. The unstable mode takes the positive real value of σ for this system ($\sigma \sim 0.2$) whilst the stable mode takes the negative real counterpart of σ ($\sigma \sim -0.2$). Rotation is clockwise around positive streamfunction contours (solid black lines) and anti-clockwise around negative streamfunction contours (dashed black lines). Yellow shading indicates positive x velocity and blue shading represents negative x velocity.

3. NUMERICAL STABILITY ANALYSIS

Given that this flow profile is analytically tractable, it may be considered unnecessary to also characterise the system stability numerically. However, this presents an ideal opportunity to test our numerical methods for assessing the modal stability of parallel shear flows, since the analytical solution is known and available for comparison.

The procedure used to numerically study the modal stability of the profile is:

1. Manipulate the perturbation equation of motion, the *Rayleigh Equation*, into an eigenproblem of the form
$$\sigma\hat{\phi} = \mathcal{A}\hat{\phi} \tag{29}$$
or, in this case,
$$\sigma\hat{\psi} = \mathcal{A}\hat{\psi} \tag{30}$$
where the operator $\mathcal{A}$ captures the z dependence of the basic state, and thus the boundary conditions.
2. Discretise the operator $\mathcal{A}$. This will also require discretising the flow profile $U(z)$.
3. Utilise inbuilt Python tools (or other numerical methods) to evaluate the eigenvalues (σ) and eigenvectors ($\hat{\psi}(z, t = 0)$) of $\mathcal{A}$.

3.1. DISCRETISED RAYLEIGH EQUATION OPERATOR

As noted in Section 2.2, the *Rayleigh Equation* is sufficient to capture the Boussinesq equations for 2 dimensional parallel shear flows. The Rayleigh Equation as stated in Equation 14 may be manipulated into an eigenvalue problem as below,

$$\sigma\hat{\psi} = (\partial_{zz} - k^2)^{-1}[-ikU(z)(\partial_{zz} - k^2) + ik(\partial_{zz}U(z)]\hat{\psi} \tag{31}$$

giving us the operator,

$$\mathcal{A} = (\partial_{zz} - k^2)^{-1}[-ikU(z)(\partial_{zz} - k^2) + ik(\partial_{zz}U(z)]. \tag{32}$$

In order to numerically determine the eigenvalues and eigenvectors of this operator, we need to represent it as a matrix. To achieve this, we define a vertical grid with grid spacing δ and number of points n_z and construct a $n_z \times n_z$ matrix operator that, when multiplied with an input vector length n_z, approximates the second derivative of the input vector with respect to the z coordinate. The selected operator $\mathbb{D}_{zz}$ approximates this second derivative using a central finite difference methodology,

$$\mathbb{D}_{zz} = \frac{1}{\delta^2}\begin{bmatrix} 1 & -2 & 1 & 0 & \dots & 0 \\ 1 & -2 & 1 & 0 & \ddots & \vdots \\ 0 & 1 & -2 & 1 & \ddots & 0 \\ 0 & 0 & 1 & -2 & \ddots & 0 \\ \vdots & \ddots & \ddots & \ddots & \ddots & 0 \\ 0 & \dots & 0 & 1 & -2 & 1 \end{bmatrix}. \tag{33}$$

The Rayleigh Equation operator $\mathcal{A}$ can then be similarly discretised as,

$$\mathcal{A} = ik(\mathbb{D}_{zz} - k^2 I)^{-1}\Big(\text{diag}(U) \cdot (\mathbb{D}_{zz} - k^2 I) - \text{diag}(\mathbb{D}_{zz} \cdot U)\Big) \tag{34}$$

where U is a vector length n_z representing the basic state velocity field (see Section 3.2) and I is the $n_z \times n_z$ identity matrix. This matrix can be constructed and its eigensolutions computed numerically.

3.2. DISCRETISED BASIC STATE

As noted in the previous section, constructing $\mathcal{A}$ requires a discrete representation of the basic state velocity profile U and it's second derivative $\partial_{zz}U$. Two pathways for producing these objects were tested:

1. Approximating the discontinuous piecewise profile (Equation 1) with a continuous $\tanh$ function,

$$U(z) = U_0 \tanh\left(\frac{z}{a}\right) \tag{35}$$

   and utilising the derivatives of this approximated profile.

2. Discretising the Equation 1 on a fine grid and numerically differentiating the discontinuous profile directly. This was anticipated to result in issues around the discontinuities in U'.

The success of these approximations are shown in Figure 4. It is evident that if a fine enough z grid is used, numerically differentiating the piecewise function directly is a viable approach and may better represent the δ-Dirac functions in $\partial_{zz}U$.

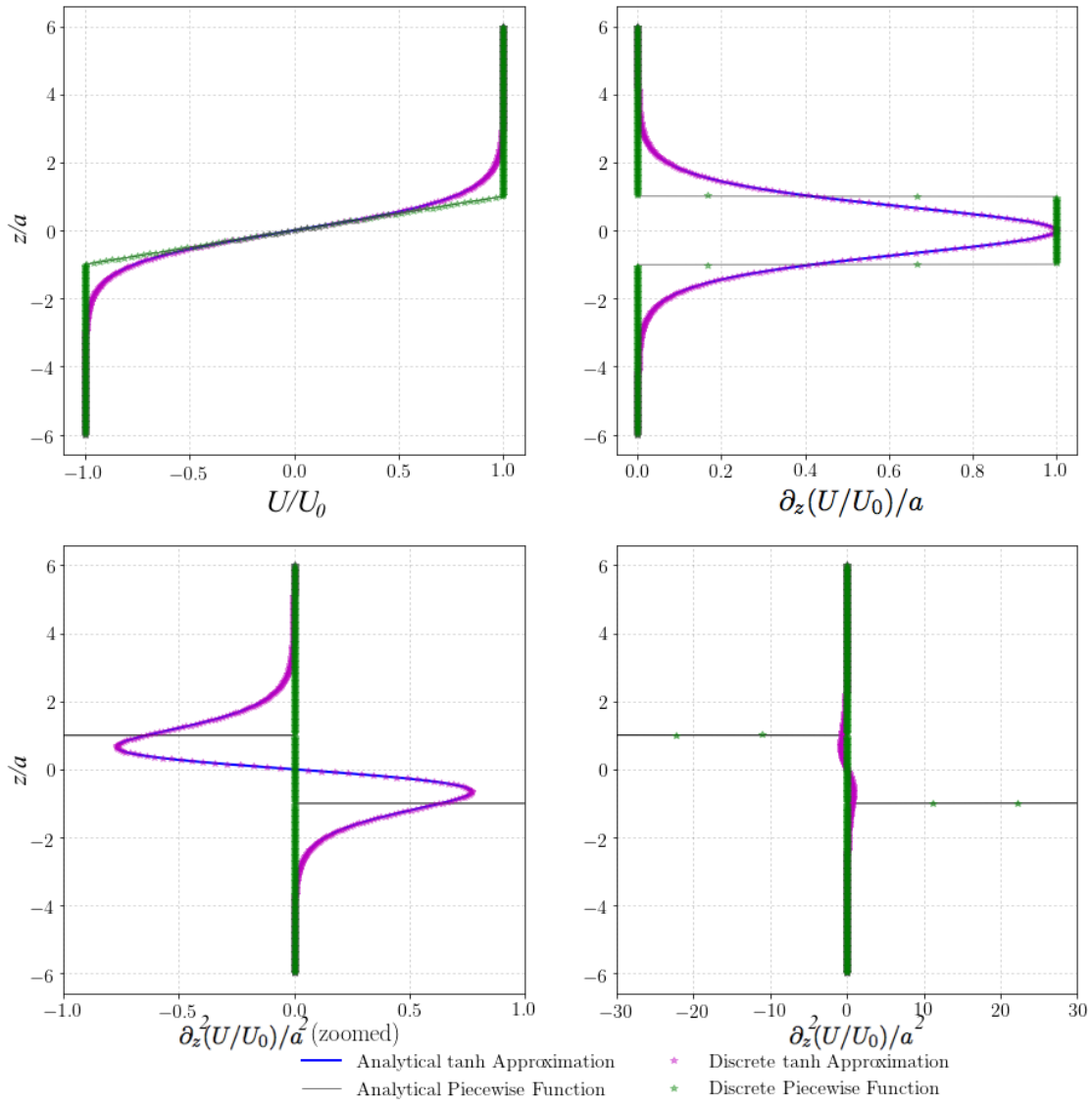

Figure 4: Discrete approximations of the piecewise linear U profile and derivatives in z. Note the analytical second derivative of the piecewise function is composed of 2 δ-Dirac functions, and that this is poorly approximated by the second derivative of the $\tanh$ approximation. In both approximations, $n_z = 401$ points were used.

3.3. SOLVING THE STABILITY EIGENPROBLEM (NUMERICAL)

To obtain numerical solutions for σ, the discretised U profiles (both $\tanh$ and piecewise) were then substituted into Equation 34 to produce a range of $\mathcal{A}$ matrices for k values between 0 and 1. The eigenvalues (σ) and corresponding eigenvectors, which take the form

$$\begin{bmatrix} \hat{\psi}_{z=0} \\ \vdots \\ \hat{\psi}_{z=n_z} \end{bmatrix}_{t=0}, \tag{36}$$

of these matrices were then computed using an inbuilt Python numpy function. The agreement between these numerically computed eigenvalues and the analytical solution for σ is shown in Figure 5. The numerical solution using the piecewise linear U profile performs remarkably well, capturing the transition from instability to stability at $ka \sim 0.639$, whilst the $\tanh$ approximation is less successful, and suggests that the basic state would remain unstable for much higher values of ka. This procedure suggests that numerical eigenproblem analysis using the Rayleigh equation can successfully capture the modal stability characteristics, but that the numerical representation of the initial velocity profile must be selected carefully.

The perturbation flow field computed using the piecewise U profile for $ka = 0.4$ is shown in Figure 6. The variables displayed are computed from the eigenvectors of our eigenproblem analysis, which provide $\hat{\psi}$ values on a z grid corresponding to a given σ at $t = 0$ as in Equation 36. The flow field illustrated is in good agreement with the unstable component of the analytical solution for $ka = 0.4$ (Figure 3) though the magnitudes are reduced, likely a consequence of setting $B = 1$ in Figure 3.

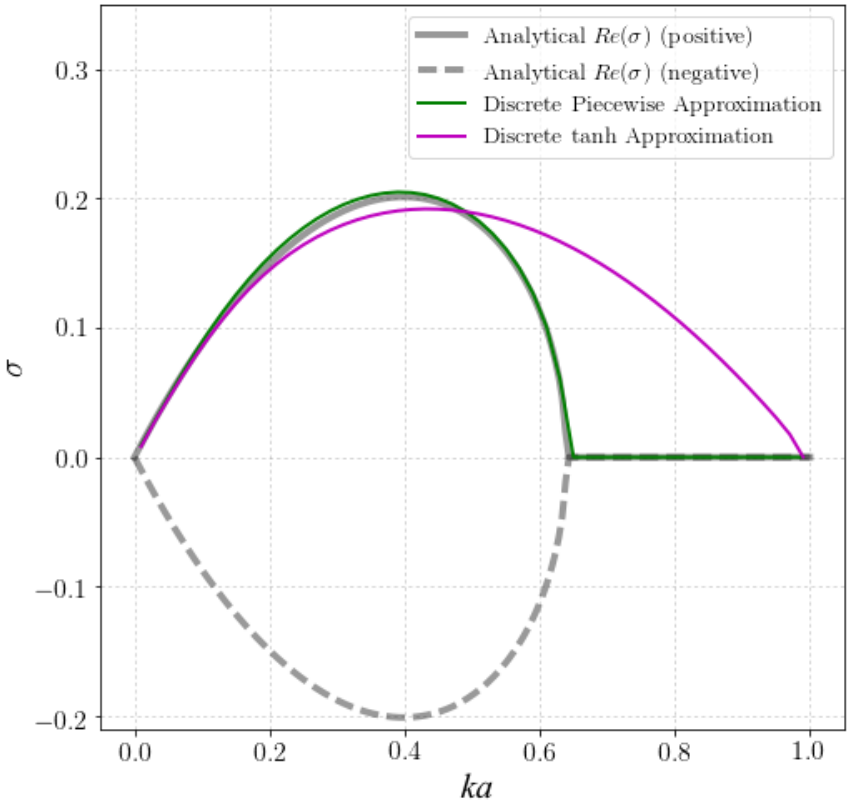

Figure 5: Numerical approximations and analytical solutions for the instability growth rate σ. Only the positive components of the eigenmodes were approximated numerically.

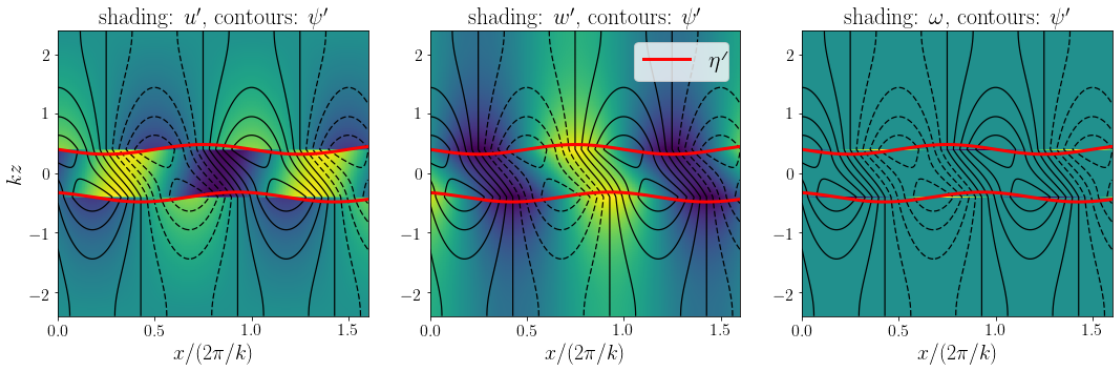

Figure 6: Plots of u', w', ψ' and $\boldsymbol{\omega}$ at $t = 0$ for the perturbation field where $U_0 = a = 1$ and $ka = 0.4$. The positive, unstable, eigenmode is selected for display.

4. Interpretation through edge wave interactions

Now that we have determined how the modal stability of this basic state changes with the lengthscale ka, we should ask: why does such a dependence exist? Why do we have instability when our shear layer is thin or the wavelength of our perturbation long, but not when the shear layer is large or the wavelength of our perturbation small? To address this question, consider a situation where a (or equivalently, k) is so large that we may effectively treat the Rayleigh profile as 2 independent flow fields, A and B (Figure 7).

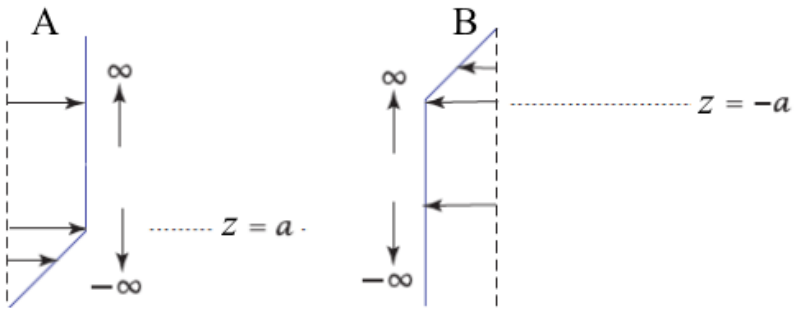

Figure 7: Two independent parallel shear flows, each containing one $\boldsymbol{\omega}$ discontinuity. This can be used to study the extreme case of $ka \to \infty$ where Rayleigh's profile well represented by two separate flows.

Taking into account standard boundary conditions at $z = \pm\infty$, the Rayleigh Equation (Equation 14) for these flows may be assumed to have solutions of the form,

$$\begin{array}{cc} \text{Flow A:} & \text{Flow B:} \\ \hat{\psi}_{A,1} = \tilde{\psi}_{A,1} e^{-k(z-a)} & \hat{\psi}_{B,1} = \tilde{\psi}_{B,1} e^{-k(z+a)}. \\ \hat{\psi}_{A,2} = \tilde{\psi}_{A,2} e^{+k(z-a)} & \hat{\psi}_{B,2} = \tilde{\psi}_{B,2} e^{+k(z+a)} \end{array} \tag{37}$$

When we further account for pressure continuity and material interface conditions at $z = \pm a$, as in Section 2, we find that these flows have the following eigenvalue solutions,

$$\begin{array}{cc} \text{Flow A:} & \text{Flow B:} \\ \sigma_A = i\left(\frac{U_0}{2a} - kU_0\right) & \sigma_B = -i\left(\frac{U_0}{2a} - kU_0\right). \end{array} \tag{38}$$

So when a is so large that the interfaces do not interact, the growth rates of perturbations at both interfaces are purely imaginary, and so these flows are modally stable. These equations characterise a phenomena called *edge waves* (Vallis, 2017). Edge waves are oscillations that propagate along internal boundaries in parallel shear flows where $\boldsymbol{\omega}$ is discontinuous, but U is continuous. In isolation, these edge waves do not lead to instability, yet we have seen in this study of the Rayleigh profile that the *interaction of numerous*

edge waves can cause instability. To get a basic, mechanistic understanding of why this is so, consider what would happen if we tried to recombine these separate flow fields A and B. Recombining the flows requires that each section experience the same perturbation field ϕ', with the same time dependence σ (recall that throughout this form of analysis we look for perturbation solutions of the form $\phi' = \hat{\phi}(z)e^{ikx+\sigma t}$), and so recombining the flows whilst retaining stable eigenvalues of the form in Equation 38 requires,

$$\sigma_A = \sigma_B = 0 \quad \text{and} \quad ka = 0.5. \tag{39}$$

This is very close to the threshold ka value, 0.639, above which the growth rate of perturbations to the Rayleigh profile ceased to be unstable. This suggests that our basic state is stable for $ka > 0.639$ because the profile effectively behaves as two independent stable flows, but it leaves us with the mystery of why Rayleigh profiles with $0.5 < ka < 0.639$ are unstable. Evidently this simple approach of combining two stable flows and seeing when the stable solution continues to hold does not capture the whole situation.

REFERENCES

Vallis, Geoffrey K. *Atmospheric and Oceanic Fluid Dynamics: Fundamentals and Large-Scale Circulation*. Cambridge University Press, 2 edition, 2017. doi: 10.1017/9781107588417.